


Coupling of acoustic phonons to spin-orbit entangled pseudospinsS.-K. Yip ^{*}*Institute of Physics, Academia Sinica, Taipei 115, Taiwan
and Institute of Atomic and Molecular Sciences, Academia Sinica, Taipei 106, Taiwan*

(Received 4 July 2023; accepted 27 September 2023; published 11 October 2023)

We consider coupling of acoustic phonons to pseudospins consisting of electronic spins locked to orbital angular momentum states. We show that a Berry phase term arises from projection onto the time-dependent lowest-energy manifold. We examine consequences on the phonon modes, particularly mode splitting, induced chirality, and Berry curvatures under an external magnetic field which Zeeman couples to the pseudospin.

DOI: [10.1103/PhysRevB.108.165116](https://doi.org/10.1103/PhysRevB.108.165116)**I. INTRODUCTION**

How phonons couple to a magnetic field has received a lot of attention recently, with particular boost due to the interest in thermal Hall effects and the question of possible phonon contributions [1–10]. In this paper, we investigate a mechanism of phonon–magnetic field coupling whereby an acoustic phonon can acquire a Berry curvature, and the otherwise degenerate phonon modes (in the absence of this coupling) would be mixed, producing chiral modes with finite frequency splitting. The general mechanism of generating such a coupling between the phonon and the magnetic field is by now well appreciated, while in the case of optical phonons in strongly ionic solids, the coupling can be directly comprehended as due to motion of the charged ions [11]; in general, it must be understood as a Berry phase effect [12–17]. Phonons are associated with the motion of the atoms or ions in the solid. The electrons, on the other hand, not only provide an effective scalar potential between the ions given in the traditional Born-Oppenheimer approximation but also carry a Berry phase factor depending on the ionic coordinates. This phase factor, after the electron degrees of freedom have been eliminated, gives rise to an effective vector potential [12–18] and hence Lorentz force for the motions of the ions or nuclei. Traditional first-principles phonon calculations in solids based on density functional theory [19] consider electron-phonon interactions only via the interatomic force constant matrix and thus miss the Berry phase contribution mentioned above, though authors of more recent works (e.g., Ref. [17]) have allowed for this contribution. The generation of gauge field on one subsystem via projecting out the other has also been discussed in other branches of physics (e.g., Refs. [20–22]).

Here, we shall consider phonons coupling to the magnetic field via spins. We shall primarily consider localized spins in the paramagnetic regime, where the spins are not ordered or even noninteracting, with finite polarization only due to the external applied magnetic field. The coupling mechanism we consider is different from those investigated in the

literature, such as magnetic anisotropy energy [23] in magnetically ordered systems or modifications of spin-spin interaction energies due to bond length or angle changes in the presence of phonons. The specific systems we shall examine are those where the spins are actually pseudospins, with electronic spins entangled with orbital angular momentum states, for example, Ru^{+3} ions in $\alpha\text{-RuCl}_3$ [3,4,6,10] or Ir^{+4} in Sr_2IrO_4 [24–27] with (Kramers degenerate) ground states well separated from excited states [28]. Systems with such strong spin-orbit entangled pseudospins themselves have gained strong recent attention due to interesting physics such as spin-orbit assisted Mott transition, unusual interaction between pseudospins, possible spin liquids, and multipolar order [29]. In the presence of the acoustic phonon, the local environment becomes time dependent. If the pseudospin is not excited, then this pseudospin must remain within the ground-state manifold though defined according to this instantaneous environment. This time dependence then generates an effective gauge field for the ionic motion. Since the pseudospin Zeeman couples to the magnetic field, direct phonon–magnetic field coupling would result, providing the mechanism we desire in the first paragraph. Explicitly, we shall be examining d -electron systems in cubic environment. However, the mechanism seems to be quite general when both crystal field splitting and strong spin-orbit coupling are present when the phonon frequencies lie within suitable frequency ranges. Since a projection into a subspace is necessary, our mechanism is only applicable for such strongly spin-orbit entangled systems.

Our mechanism to be discussed here is distinct from the one which has been investigated also for spin-orbit entangled pseudospins particularly for f -electron systems (e.g., Refs. [30–33]) coupling to optical phonons. There, the coupling, termed magnetoelastic interaction in Refs. [30–33] (but to be distinguished from magnetoelastic couplings which has been discussed in magnetostriction or for acoustic waves in, e.g., Refs. [23,34]), arises from the modification of crystal fields acting on the pseudospins in the presence of the optical phonons. These phonon-pseudospin couplings are parameterized by coupling constants which describe thus the extent that the crystal fields are modified due to the displacements of the ions surrounding the pseudospin under discussion. In

^{*}yip@phys.sinica.edu.tw

this mechanism, the splitting of degenerate phonon modes by the magnetic field is generated by virtual transitions between different energy manifolds [30,31]. In contrast, our mechanism arises from phase factors generated from projection onto the time-dependent pseudospin ground state manifold. As we shall see, the coupling constant depends on the information entirely of the ground-state manifold and in fact a factor related to the geometric information on the structure of the pseudospin.

The structure of the rest of this paper is as follows. In Sec. II, we introduce our specific model and then derive the phonon-pseudospin coupling. The effect of this coupling on the sound modes frequencies is evaluated in Sec. III. In Sec. IV, we evaluate the Berry curvatures. We end with some order-of-magnitude estimates and discussions in Sec. V.

II. MODEL

To be specific, consider Ir^{+4} ions in Sr_2IrO_4 or Ru^{+3} ions in RuCl_3 , both with five d electrons (see, e.g., Refs. [24–27]). In both cases, the ions are situated within an approximately cubic environment formed by the O^{2-} and Cl^{-1} ions, respectively. The d -electron energy levels are crystal-field split into t_{2g} and e_{2g} manifolds. Only the t_{2g} manifold consisting of the orbitals usually labeled as xy , yz , and zx are relevant and, together with the electronic spin \uparrow and \downarrow degree of freedom, form six levels. The spin-orbit interaction further splits these six levels into one quartet, usually labeled as $j_{\text{eff}} = \frac{3}{2}$, which are occupied, and another Kramer's doublet, usually labeled as $j_{\text{eff}} = \frac{1}{2}$, which is singly occupied. We shall write the wave functions for the two levels in this doublet as [35]

$$\begin{aligned} |\uparrow\rangle &= \frac{-i}{\sqrt{3}} [|xy \uparrow\rangle + |yz \downarrow\rangle + i |xz \downarrow\rangle], \\ |\downarrow\rangle &= \frac{i}{\sqrt{3}} [|xy \downarrow\rangle - |yz \uparrow\rangle + i |xz \uparrow\rangle], \end{aligned} \quad (1)$$

forming a time-reversal pair (we use the convention, under time-reversal, $|\uparrow\rangle \rightarrow |\downarrow\rangle$, $|\downarrow\rangle \rightarrow -|\uparrow\rangle$, and similarly, $|\uparrow\rangle \rightarrow |\downarrow\rangle$, $|\downarrow\rangle \rightarrow -|\uparrow\rangle$). In the absence of phonons, the orbital parts of the wave functions (xy , yz , zx) as well as the spin parts (\uparrow , \downarrow) are defined according to fixed axes with respect to the crystal in equilibrium.

Before we consider phonons, let us first note a few relations which we shall use. Denoting the electronic spin operator by $\vec{s} = \frac{1}{2}\vec{\sigma}$, where $\vec{\sigma}$ are Pauli matrices operating on the \uparrow and \downarrow space, and \vec{L} the orbital angular momentum operator, their projections onto the subspace of Eq. (1) are [36]

$$\vec{s} = -\frac{1}{6}\vec{\tau}, \quad \vec{L} = -\frac{2}{3}\vec{\tau}, \quad (2)$$

where $\vec{\tau}$ are Pauli matrices within the \uparrow , \downarrow space. The energy change under a magnetic field \vec{B} , $\mu_B(\vec{L} + 2\vec{s}) \cdot \vec{B}$ (with μ_B the Bohr magneton), with the operators projected again onto this subspace (i.e., ignoring thus other contributions), would then be

$$E_Z = \mu_B \left(-\frac{2}{3} - \frac{1}{3} \right) \vec{\tau} \cdot \vec{B} \equiv -g\mu_B \frac{\vec{\tau}}{2} \cdot \vec{B}, \quad (3)$$

with an effective g factor of 2 [25,26]. In the first equality of Eq. (3), $-\frac{2}{3}$ arises from \vec{L} , and $-\frac{1}{3} = 2 \times (-\frac{1}{6})$ arises from

2 \vec{s} . Equation (2) implies

$$\vec{L} + \vec{s} = -\frac{5}{6}\vec{\tau}, \quad (4)$$

a result which we shall use later.

A. Phonon-pseudospin coupling

Consider a long-wavelength acoustic phonon, with a spatial and time-dependent displacement vector $\vec{\xi}(\vec{x}, t)$. For simplicity, we shall consider a cubic crystal and remark on modifications for other symmetries later. As is well known, we can decompose this into three components: $\vec{\nabla} \cdot \vec{\xi}$, $\frac{1}{2}\vec{\nabla} \times \vec{\xi}$, and the tensor $\frac{1}{2}(\frac{\partial \xi_i}{\partial x_j} + \frac{\partial \xi_j}{\partial x_i}) - \frac{1}{3}\delta_{ij}\vec{\nabla} \cdot \vec{\xi}$, corresponding to an isotropic expansion (compression), rotation, and anisotropic deformation, respectively [37]. Under low-energy excitations of the crystal [28], the electronic state $|\Psi\rangle$ of our ion under consideration should still be within the manifold described by Eq. (1), though in a frame specified by the local environment. Hence, at an instantaneous time t , we should have (up to small terms describing the excitations to higher-energy levels)

$$|\Psi(t)\rangle = \alpha'_\uparrow(t) |\uparrow'(t)\rangle + \alpha'_\downarrow(t) |\downarrow'(t)\rangle, \quad (5)$$

where $|\uparrow'(t)\rangle$ [$|\downarrow'(t)\rangle$] are states given by Eq. (1) except with $x, y, z, |\uparrow\rangle, |\downarrow\rangle$ replaced by $x', y', z', |\uparrow'\rangle, |\downarrow'\rangle$ rotated from the former by $\vec{\Theta}(t) \equiv \frac{1}{2}\vec{\nabla} \times \vec{\xi}(t)$. (The isotropic compression and anisotropic deformation would not affect what we would be discussing below [38] and shall be ignored from now on.) Suppose that our ion is under an external field \vec{B} , and let \vec{B}' be the value of this field in the abovementioned rotating frame. The Schrödinger equation of motion for $|\Psi\rangle$, employing Eq. (5) and noting the time dependence of the basis function $|\uparrow'(t)\rangle, |\downarrow'(t)\rangle$, implies

$$\begin{aligned} i\frac{\partial}{\partial t} \begin{pmatrix} \alpha'_\uparrow \\ \alpha'_\downarrow \end{pmatrix} &= -g\mu_B \vec{B}'(t) \cdot \frac{\vec{\tau}}{2} \begin{pmatrix} \alpha'_\uparrow \\ \alpha'_\downarrow \end{pmatrix} \\ &+ \begin{pmatrix} -i\langle \uparrow' | \frac{\partial}{\partial t} | \uparrow' \rangle & -i\langle \uparrow' | \frac{\partial}{\partial t} | \downarrow' \rangle \\ -i\langle \downarrow' | \frac{\partial}{\partial t} | \uparrow' \rangle & -i\langle \downarrow' | \frac{\partial}{\partial t} | \downarrow' \rangle \end{pmatrix} \begin{pmatrix} \alpha'_\uparrow \\ \alpha'_\downarrow \end{pmatrix}. \end{aligned} \quad (6)$$

Here, $\vec{\tau}$, which rigorously should have been denoted as $\vec{\tau}'$, are Pauli matrices in the \uparrow', \downarrow' subspace, but we shall not make this distinction in notations for simplicity. Since $|\uparrow'(t)\rangle = \exp[-i\vec{\Theta} \cdot (\vec{L} + \vec{s})] |\uparrow\rangle \approx [1 - i\vec{\Theta} \cdot (\vec{L} + \vec{s})] |\uparrow\rangle$, the time derivatives can be evaluated as, e.g., $-i\langle \uparrow' | \frac{\partial}{\partial t} | \uparrow' \rangle = -(\frac{\partial \vec{\Theta}}{\partial t}) \cdot [(\langle \uparrow' | (\vec{L} + \vec{s}) | \uparrow' \rangle)]$. Using Eq. (4) (and ignoring terms $\propto \vec{\Theta} \times \frac{\partial \vec{\Theta}}{\partial t}$, which arise due to the difference between the primed and unprimed \uparrow and \downarrow space), we obtain

$$i\frac{\partial}{\partial t} \begin{pmatrix} \alpha'_\uparrow \\ \alpha'_\downarrow \end{pmatrix} = \left[-g\mu_B \vec{B}'(t) \cdot \frac{\vec{\tau}}{2} + \frac{5}{6} \frac{\partial \vec{\Theta}}{\partial t} \cdot \vec{\tau} \right] \begin{pmatrix} \alpha'_\uparrow \\ \alpha'_\downarrow \end{pmatrix}. \quad (7)$$

It would be more convenient to have an equation of motion directly involving \vec{B} instead. We observe that $\vec{B}' = \vec{B} - \vec{\Theta} \times \vec{B}$, and hence, $\vec{B}' \cdot \vec{\tau} = \exp(i\frac{\vec{\Theta}}{2} \cdot \tau) \vec{B} \cdot \vec{\tau} \exp(-i\frac{\vec{\Theta}}{2} \cdot \tau)$.

Introducing

$$\begin{pmatrix} \tilde{\alpha}'_{\uparrow} \\ \tilde{\alpha}'_{\downarrow} \end{pmatrix} = \exp\left(-i\frac{\tilde{\Theta}}{2} \cdot \tau\right) \begin{pmatrix} \alpha'_{\uparrow} \\ \alpha'_{\downarrow} \end{pmatrix}, \quad (8)$$

we finally obtain

$$i\frac{\partial}{\partial t} \begin{pmatrix} \tilde{\alpha}'_{\uparrow} \\ \tilde{\alpha}'_{\downarrow} \end{pmatrix} = \left[-\frac{g\mu_B}{2}\vec{B} + \frac{4}{3}\frac{\partial\tilde{\Theta}}{\partial t}\right] \cdot \vec{\tau} \begin{pmatrix} \tilde{\alpha}'_{\uparrow} \\ \tilde{\alpha}'_{\downarrow} \end{pmatrix}, \quad (9)$$

where we have again dropped a term involving second powers in Θ . Here, $\frac{4}{3}$ arises from $\frac{1}{2} - (-\frac{5}{6})$, thus is due to the difference between the rotational matrix for ordinary spin- $\frac{1}{2}$ and our pseudospin [Eq. (4)]. The direction of the pseudospin, defined as the expectation value of $\vec{\tau}$ with the spin wave function $(\tilde{\alpha}'_{\uparrow}, \tilde{\alpha}'_{\downarrow})$, is given by

$$\frac{\partial}{\partial t}\hat{\tau} = \hat{\tau} \times \left[\tilde{\omega}_0 + r\frac{\partial\tilde{\Theta}}{\partial t}\right] = \hat{\tau} \times \left[\tilde{\omega}_0 + \frac{r}{2}\left(\nabla \times \frac{\partial\vec{\xi}}{\partial t}\right)\right], \quad (10)$$

with $\tilde{\omega}_0 = g\mu_B\vec{B}$ and $r = -\frac{8}{3}$. The former is the standard precession due to the external field, and the second extra term is due to the rotational properties of our basis functions derived above.

B. Lagrangian

Now we construct the Lagrangian for the coupled phonon and pseudospin system. To simplify the writing, when no confusion arises, we shall often just write spin for the pseudospin.

First, the acoustic phonon alone can be described by the Lagrangian density:

$$L_{0,ph} = \frac{1}{2}\rho_M \left(\frac{\partial\xi_j}{\partial t}\right)^2 - U_{\text{elastic}}, \quad (11)$$

where $U_{\text{elastic}} = \frac{1}{2}[\lambda_1(\frac{\partial\xi_j}{\partial x_i}\frac{\partial\xi_j}{\partial x_i}) + \lambda_2\frac{\partial\xi_j}{\partial x_j}\frac{\partial\xi_l}{\partial x_l}]$ is the elastic energy density. Here, ρ_M is the mass density (dimension mass times inverse volume), and sums over repeated indices are implicit. We have also ignored a term $\lambda_3(\frac{\partial\xi_j}{\partial x_j}\frac{\partial\xi_l}{\partial x_l})$, which is allowed in cubic symmetry for simplicity. Its effects will be discussed later. Under this simplification, for a system without coupling to spin, sound velocities are independent of direction of propagation \hat{q} , with longitudinal and transverse sound velocities given by $v_L = [(\lambda_1 + \lambda_2)/\rho_M]^{1/2}$ and $v_T = [\lambda_1/\rho_M]^{1/2}$, respectively.

For the spin, first, we recall that, for a spin S under a magnetic field along \hat{z} , the Lagrangian can be written as [39] $L_s = g\mu_B S B \cos\theta + S \cos\theta \frac{\partial\phi}{\partial t}$, where θ and ϕ are the angles for the spin direction in spherical coordinates, the first term being from the Zeeman energy and the second a Berry phase term. To produce the equation of motion, Eq. (10), we need only to replace $g\mu_B S B \cos\theta$ by $\frac{\vec{\tau}}{2} \cdot [g\mu_B\vec{B} + \frac{r}{2}(\nabla \times \frac{\partial\vec{\xi}}{\partial t})]$ (now specializing to pseudospin $\frac{1}{2}$). The last term allows us to identify the pseudospin-phonon coupling.

The Lagrangian $L = L_{ph} + L_s + L_{ph-s}$ is a sum of the phonon term in Eq. (11), the spin term, and the phonon-spin

coupling term. We then have, for a net effective spin density ρ_s per unit volume,

$$L_s = \rho_s \frac{1}{2} \left[g\mu_B \vec{B} \cdot \hat{\tau} + \cos\theta \frac{\partial\phi}{\partial t} \right], \quad (12)$$

$$L_{ph-s} = \frac{r\rho_s}{4} \left[\hat{\tau} \cdot \left(\nabla \times \frac{\partial\vec{\xi}}{\partial t} \right) \right], \quad (13)$$

with $\hat{\tau}$ the net (pseudo-)spin direction. The phonon-pseudospin coupling is dictated by the factor r derived in the last subsection. As is evident from our derivation above, this coupling arises from the Berry phase due to the rotating frame of reference for the pseudospin in the presence of the transverse acoustic phonon. We remind the readers here that this coupling thus has an entirely different origin from the magnetoelastic coupling discussed by, e.g., Ref. [23] for magnetic materials, which describes the change in magnetic energies in the presence of stress.

C. Effective equation of motion

The equation of motion for $\hat{\tau}$ was already obtained in Eq. (10), which reads, after Fourier transform and linearizing about the equilibrium, where $\hat{\tau} = \hat{z}$,

$$-i\omega\hat{\tau}(\omega, \vec{q}) = \omega_0(\hat{\tau} \times \hat{z}) + \frac{r\omega}{2}[\hat{z} \times (\vec{q} \times \vec{\xi})], \quad (14)$$

where \vec{q} is the wave vector and ω the angular frequency.

The equation of motion for the displacement is

$$\rho_M \omega^2 \xi_j - \frac{r\omega}{4} \rho_s (\vec{q} \times \hat{\tau})_j = \lambda_1 q^2 \xi_j + \lambda_2 q_l (q_j \xi_l). \quad (15)$$

We now study the consequences of Eqs. (14) and (15). Equation (14) implies that $\hat{\tau}_z$ is just a constant. The components orthogonal to the field direction ($j = x, y$) obey

$$\tau_j = \frac{r\omega/2}{\omega_0^2 - \omega^2} \{ \omega_0 (\vec{q} \times \vec{\xi})_j - i\omega [\hat{z} \times (\vec{q} \times \vec{\xi})]_j \}. \quad (16)$$

Putting this into Eq. (15) gives us the equation of motion entirely expressed in terms of ξ_j :

$$\begin{aligned} 0 = & \rho_M \omega^2 \xi_j - [\lambda_1 q^2 \xi_j + \lambda_2 q_l (q_j \xi_l)] \\ & - \frac{r^2 \rho_s}{8} \frac{\omega_0 \omega^2}{\omega_0^2 - \omega^2} \{ -q_z^2 \xi_j + q_z q_j \xi_z + [q_z (q_l \xi_l) - q^2 \xi_z] \delta_{jz} \} \\ & - i \frac{r^2 \rho_s}{8} \frac{\omega^3}{\omega_0^2 - \omega^2} q_z (\vec{q} \times \vec{\xi})_j. \end{aligned} \quad (17)$$

Coupling of the pseudospin to the phonon results in the last two new terms. Here, the factor $\delta_{jz} = 1$ if $j = z$ and vanishes otherwise. We note the factor q_z in the last term, which is generated from the last term in Eq. (16). This factor reflects the fact that the time-dependent parts of τ only have x and y components.

We now analyze Eq. (17) in two different limits.

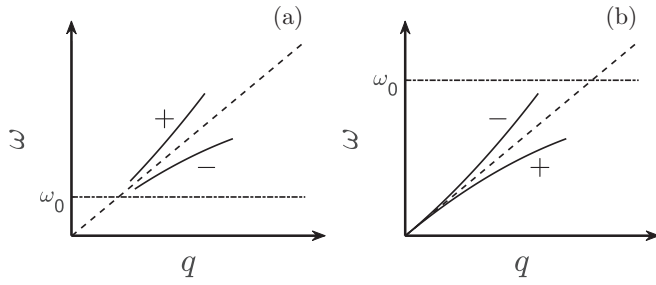


FIG. 1. Schematic dispersions for the transverse phonon modes for $q_z > 0$. + (−) labels right (left) circularly or elliptically polarized. For $q_z < 0$, the \pm labels in the above figures have to be reversed. (a) Antiadiabatic regime and (b) adiabatic.

III. SOUND MODES

A. Small magnetic field: Antiadiabatic regime

For small fields, ω_0 is much smaller than the phonon frequencies, and Eq. (17) approximately reads

$$0 = \rho_M \omega^2 \xi_j - [\lambda_1 q^2 \xi_j + \lambda_2 q_l (q_j \xi_l)] + i \frac{r^2 \rho_s}{8} \omega q_z (\vec{q} \times \vec{\xi})_j. \quad (18)$$

Longitudinal sound, with ξ parallel to \vec{q} , is not affected. Physically, there is no rotation of the environment surrounding the pseudospin in this case. The two polarizations of the transverse sound are coupled via the spins, turning them into circular polarized ones. Writing $\vec{\xi} = \xi_\theta \hat{\theta} + \xi_\phi \hat{\phi}$, we get

$$\begin{pmatrix} \omega^2 - q^2 v_T^2 & -i \frac{\rho_s r^2}{8 \rho_M} \omega q^2 \cos \theta_q \\ +i \frac{\rho_s r^2}{8 \rho_M} \omega q^2 \cos \theta_q & \omega^2 - q^2 v_T^2 \end{pmatrix} \begin{pmatrix} \xi_\theta \\ \xi_\phi \end{pmatrix} = 0. \quad (19)$$

Here, θ_q is the angle between \hat{q} and \hat{z} . To the lowest order in the phonon-pseudospin coupling, the frequencies are given by

$$\omega_\pm = q v_T [1 \pm Z \cos \theta_q], \quad (20)$$

for the modes with right $[(\xi_\theta, \xi_\phi) \propto (1, i)]$ and left $[(\xi_\theta, \xi_\phi) \propto (1, -i)]$ circular polarization, with Z a q -dependent

$$\begin{pmatrix} \omega^2 - q^2 v_T^2 + \frac{\rho_s r^2}{8 \rho_M \omega_0} q^2 \omega^2 & i \frac{\rho_s r^2}{8 \rho_M \omega_0} \omega^3 q^2 \cos \theta_q \\ -i \frac{\rho_s r^2}{8 \rho_M \omega_0} \omega^3 q^2 \cos \theta_q & \omega^2 - q^2 v_T^2 + \frac{\rho_s r^2}{8 \rho_M \omega_0} q^2 \omega^2 \cos^2 \theta_q \end{pmatrix} \begin{pmatrix} \xi_\theta \\ \xi_\phi \end{pmatrix} = 0. \quad (23)$$

For θ_q not too close to 0 or π , we can ignore the off-diagonal terms in this matrix equation, as they are second order in ω_0^{-1} . We obtain two nondegenerate modes with frequencies $\omega = q v_T (1 + X)^{-1/2}$ (for $\vec{\xi}$ along $\hat{\theta}$) and $\omega = q v_T / (1 + X \cos^2 \theta_q)^{-1/2}$ (for $\vec{\xi}$ along $\hat{\phi}$). Here, $X \equiv \frac{\rho_s r^2 q^2}{8 \rho_M \omega_0}$ is a q -dependent dimensionless parameter. Thus, the mode with $\vec{\xi}$ along $\hat{\theta}$ has a lower frequency than the one with $\hat{\phi}$ due to the coupling to the pseudospin. For $\theta_q = 0$ or π , these two modes are degenerate up to ω_0^{-1} . The off-diagonal term then turns these transverse modes to circularly polarized. For $\theta_q = 0$, the modes with $(\xi_\theta, \xi_\phi) \propto (1, \pm i)$ have frequencies roughly given by $\omega \approx q v_T (1 + X)^{-1/2} [1 \mp X_2]$, with the dimensionless parameter $X_2 \equiv \frac{\rho_s r^2 q^2}{16 \rho_M \omega_0} \frac{q v_T}{\omega_0}$. Note that both X and X_2 are increasing functions of q . Like the case in

dimensionless parameter:

$$Z \equiv \frac{\rho_s r^2 q}{16 \rho_M v_T}. \quad (21)$$

Thus, the fractional splitting increases with q , reflecting that a shorter wavelength implies a larger rotation motion of the lattice $\vec{q} \times \vec{\xi}$ and hence a stronger coupling to our pseudospin. This is different from a naïve picture of hybridization between the phonon modes with the Larmor precession of the spins, where the induced splitting would decrease with increasing frequencies away from ω_0 . From Eq. (20), we see that, for $q_z > 0$, the lower (higher) frequency mode is left (right)-circularly polarized. The reverse is the case if $q_z < 0$. See Fig. 1(a).

B. Low frequency: Adiabatic regime

For very small q , the phonon frequency $\sim q v_T$ is much smaller than ω_0 . In this case, the effective equation of motion for the phonon coordinate can be written as

$$0 = \rho_M \omega^2 \xi_j - [\lambda_1 q^2 \xi_j + \lambda_2 q_l (q_j \xi_l)] - \frac{r^2 \rho_s \omega^2}{8 \omega_0} \{ -q_z^2 \xi_j + q_z q_j \xi_z + [q_z (q_l \xi_l) - q^2 \xi_z] \delta_{jz} \} - i \frac{r^2 \rho_s}{8} \frac{\omega^3}{\omega_0^2} q_z (\vec{q} \times \vec{\xi})_j. \quad (22)$$

Note the sign differences between the last terms of Eqs. (18) and (22) in two different frequency regimes, like the case of, e.g., a driven harmonic oscillator for the above versus below resonance. Formally, the last term is one higher order in ω_0^{-1} than the second last, but we shall explain shortly why we keep this term. Longitudinal sound is again unaffected. The eigenvector has $\vec{\xi}$ parallel to \vec{q} , as can be checked by multiplying Eq. (22) by q_j and the sum over j (there is no contribution from either the last or second-last terms). The transverse sounds obey

Sec. III A, the sign in front of X_2 in this expression for ω needs to be reversed for $\theta_q = \pi$. Note that $X_2 \ll X$ since we are now considering $q v_T \ll \omega_0$ and also that the circular polarization for the higher-frequency mode is opposite to the antiadiabatic case for a given \hat{q} . For general θ , the modes are elliptically polarized. See Fig. 1(b).

IV. BERRY CURVATURE

We here discuss the Berry curvature for the phonon modes. Our methodology here closely follows Ref. [40] and the supplemental materials of Ref. [41]. In the Appendix, we collect some of the relevant formulas. We shall again first investigate the small magnetic field regime (Sec. IV A) and then the high magnetic one (Sec. IV B). The second regime is

included here for completeness, but the information therein is not essential for our final Discussion section, so readers can choose to skip to Sec. IV B.

A. Antiaibiatic

The Lagrangian density that reproduces the equation of motion, Eq. (18), can easily be found:

$$L = L_{0,ph} + \frac{r^2 \rho_s}{16} \epsilon_{jkl} \left(\frac{\partial^2 \xi_j}{\partial z \partial x_k} \right) \left(\frac{\partial \xi_l}{\partial t} \right). \quad (24)$$

The last term, in the form of an effective Lorentz force, might have been expected from phenomenological grounds. An initial guess might be a term proportional to $\hat{z} \cdot (\vec{\xi} \times \frac{\partial \vec{\xi}}{\partial t})$: this term does arise in the case of optical phonons [32,33,42], but here, this is not acceptable since the appearance of $\vec{\xi}$ violates translational invariance. Instead, in Eq. (24), a second-order spatial derivative appears, like what has been discussed in Refs. [13,41], though in our case, the precise form, as derived in Sec II, is different here.

The conjugate momentum Π_j is given by

$$\Pi_j \equiv \frac{\partial L}{\partial \dot{\xi}_j} = \rho_M \left(\frac{\partial \xi_j}{\partial t} \right) - \frac{r^2 \rho_s}{16} \epsilon_{jkl} \left(\frac{\partial^2 \xi_l}{\partial z \partial x_k} \right), \quad (25)$$

with the equation of motion, Eq. (18), just the same as $\frac{\partial \Pi_j}{\partial t} = \frac{\partial L}{\partial \xi_j}$. After Fourier transforming the spatial coordinates, these

$$\omega \begin{pmatrix} u_\theta \\ u_\phi \\ v_\theta \\ v_\phi \end{pmatrix} = \begin{pmatrix} -iZqv_T \cos \theta_q & -i\lambda_1 q^2 & & \\ +iZqv_T \cos \theta_q & & -i\lambda_1 q^2 & \\ i\rho_M & & -iZqv_T \cos \theta_q & \\ & i\rho_M & iZqv_T \cos \theta_q & \end{pmatrix} \begin{pmatrix} u_\theta \\ u_\phi \\ v_\theta \\ v_\phi \end{pmatrix}. \quad (30)$$

The right (left)-circularly polarized mode has eigenvector [normalized according to Eq. (A8)]:

$$\left[\frac{(\rho_M q v_T)^{1/2}}{2}, \pm \frac{i(\rho_M q v_T)^{1/2}}{2}, \frac{i}{2(\rho_M q v_T)^{1/2}}, \mp \frac{1}{2(\rho_M q v_T)^{1/2}} \right], \quad (31)$$

with frequencies $\omega = qv_T(1 \pm Z \cos \theta_q)$ [c.f. Eq. (20)] and curvature $\vec{\Omega}_B = \pm \hat{q}/q^2$.

B. Adiabatic

In this regime, Eq. (22) indicates that the equation for the frequency is cubic. This creates complications if we want to treat the problem in the same way as in the last subsection. However, since we are treating the pseudospin-phonon coupling as small, we can simplify the problem by noting the fact that, since the last term in Eq. (22) is thus already small, we can replace ω^2 there by the unperturbed transverse sound frequency $(qv_T)^2$ (transverse since the last term affects only the transverse modes). Thus, we now consider the effective equation of motion:

$$0 = \rho_M \omega^2 \xi_j - [\lambda_1 q^2 \xi_j + \lambda_2 q_l (q_j \xi_l)] - \frac{r^2 \rho_s \omega^2}{8\omega_0} \left\{ -q_z^2 \xi_j + q_z q_j \xi_z + [q_z (q_l \xi_l) - q^2 \xi_z] \delta_{jz} \right\} - i \frac{r^2 \rho_s}{8} \frac{\omega (qv_T)^2}{\omega_0^2} q_z (\vec{q} \times \vec{\xi})_j. \quad (32)$$

This equation reproduces the sound velocities discussed near the end of Sec. III B, and we can check that the displacement eigenvectors found below are proportional to those found there.

The Lagrangian density that reproduces this equation of motion can easily be found:

$$L = L_{0,ph} + \frac{r^2 \rho_s}{8\omega_0} \left[\frac{1}{2} \left(\frac{\partial^2 \xi_l}{\partial z \partial t} \right)^2 - \left(\frac{\partial^2 \xi_z}{\partial z \partial t} \right) \left(\frac{\partial^2 \xi_l}{\partial x_l \partial t} \right) + \frac{1}{2} \left(\frac{\partial^2 \xi_z}{\partial x_l \partial t} \right)^2 \right] + \frac{r^2 \rho_s v_T^2}{16\omega_0^2} \nabla^2 \vec{\xi} \cdot \vec{\nabla} \times \left(\frac{\partial^2 \vec{\xi}}{\partial z \partial t} \right). \quad (33)$$

two equations can be written in matrix form:

$$\frac{\partial}{\partial t} \begin{pmatrix} \rho_M \hat{1} & 0 \\ \rho_M \Omega & \hat{1} \end{pmatrix} \begin{pmatrix} \xi \\ \Pi \end{pmatrix} = \begin{pmatrix} -\rho_M \Omega & \hat{1} \\ -\mathcal{Q} & 0 \end{pmatrix} \begin{pmatrix} \xi \\ \Pi \end{pmatrix}, \quad (26)$$

where Ω , \mathcal{Q} , and $\hat{1}$ are 3×3 matrices: $\Omega \equiv Z(qv_T) \cos \theta_q \hat{\Omega}$, with Z defined in Eq. (21), $\hat{\Omega}_{jk} \equiv -\epsilon_{jkl} \hat{q}_l$, $\mathcal{Q}_{jk} \equiv \lambda_1 q^2 \delta_{jk} + \lambda_2 q_j q_k$, and $\hat{1}_{jk} = \delta_{jk}$.

Equation (26) can be rewritten as

$$\frac{\partial}{\partial t} \begin{pmatrix} \xi \\ \Pi \end{pmatrix} = -i\mathcal{S} \begin{pmatrix} \xi \\ \Pi \end{pmatrix}, \quad (27)$$

with ξ , Π column matrices consisting of elements $\xi_{x,y,z}$ and $\Pi_{x,y,z}$, and \mathcal{S} a 6×6 matrix given by

$$\mathcal{S} = \begin{pmatrix} -i\Omega & i/\rho_M \\ -i\mathcal{Q} & -i\Omega \end{pmatrix}, \quad (28)$$

where rigorously speaking, the lower left element should have been $-i\mathcal{Q} + i\rho_M \Omega^2$, and we have taken the simpler form since Ω^2 is second order in $1/\omega_0$ and hence higher order than the other terms we kept.

Following Ref. [41], we search for the row vectors (\vec{u}, \vec{v}) which satisfy, for positive frequencies ω ,

$$\omega(\vec{u}, \vec{v}) = (\vec{u}, \vec{v})\mathcal{S}. \quad (29)$$

Once (\vec{u}, \vec{v}) 's are found, the Berry curvatures $\vec{\Omega}_B$ can then be evaluated via the formulas collected in Appendix B. For the longitudinal mode, $(\vec{u}, \vec{v}) = (u_q \hat{q}, v_q \hat{q})$. The transverse modes can be more easily written in terms of $u_{\theta,\phi}$ and $v_{\theta,\phi}$ defined via $\vec{u} = u_\theta \hat{\theta} + u_\phi \hat{\phi}$ and similarly for \vec{v} . They obey (observe that $\hat{\theta} \hat{\Omega} = -\hat{\phi}$ and $\hat{\phi} \hat{\Omega} = \hat{\theta}$)

Carrying out the same procedure as in the last subsection, we obtain

$$\frac{\partial}{\partial t} \begin{bmatrix} \rho_M(1 + X\hat{\Lambda}) & 0 \\ -\rho_M\tilde{\Omega} & 1 \end{bmatrix} \begin{pmatrix} \xi \\ \Pi \end{pmatrix} = \begin{pmatrix} \rho_M\tilde{\Omega} & 1 \\ -Q & 0 \end{pmatrix} \begin{pmatrix} \xi \\ \Pi \end{pmatrix}, \quad (34)$$

where $\tilde{\Omega} \equiv X_2 q v_T \cos \theta_q \hat{\Omega}$ (dimension frequency), with X, X_2 defined in Sec. III B and $\hat{\Omega}_{jk} Q_{jk}$ already defined in Sec. IV A:

$$\hat{\Lambda} \equiv \begin{pmatrix} \hat{q}_z^2 & 0 & -\hat{q}_x \hat{q}_z \\ 0 & \hat{q}_z^2 & -\hat{q}_y \hat{q}_z \\ -\hat{q}_z \hat{q}_x & -\hat{q}_z \hat{q}_y & q_x^2 + q_y^2 \end{pmatrix}. \quad (35)$$

We have again Eq. (27), now with

$$\mathcal{S} = \begin{pmatrix} i[1 + X\hat{\Lambda}]^{-1}\tilde{\Omega} & i/\rho_M[1 + X\hat{\Lambda}]^{-1} \\ -iQ + i\rho_M\tilde{\Omega}[1 + X\hat{\Lambda}]^{-1}\tilde{\Omega} & i\tilde{\Omega}[1 + X\hat{\Lambda}]^{-1} \end{pmatrix}, \quad (36)$$

which in accordance with our approximations, the second term in the lower left element can be dropped.

We can solve for the eigenvectors (\vec{u}, \vec{v}) as before. It is useful to note the vector relations $\hat{q}\hat{\Lambda} = 0$, $\hat{\theta}\hat{\Lambda} = \hat{\theta}$, and $\hat{\phi}\hat{\Lambda} = \cos^2 \theta_q \hat{\phi}$. Once more, for longitudinal modes, $(\vec{u}, \vec{v}) = (u_q \hat{q}, v_q \hat{q})$ is unaffected by the pseudospin. If θ_q is not too close to 0 or π , in the first approximation, we can ignore the effects of $\tilde{\Omega}$. The modes are thus linearly polarized with either \vec{u}, \vec{v} entirely along $\hat{\theta}$ or $\hat{\phi}$ with frequencies already given in Sec. III B. The normalized eigenvectors are, respectively,

$$(u_\theta, v_\theta)_0 = \left[\frac{(\rho_M q v_T)^{1/2} (1 + X)^{1/4}}{\sqrt{2}}, \frac{i}{\sqrt{2}(\rho_M q v_T)^{1/2} (1 + X)^{1/4}} \right], \quad (37)$$

and

$$(u_\phi, v_\phi)_0 = \left[\frac{(\rho_M q v_T)^{1/2} (1 + X \cos^2 \theta_q)^{1/4}}{\sqrt{2}}, \frac{i}{\sqrt{2}(\rho_M q v_T)^{1/2} (1 + X \cos^2 \theta_q)^{1/4}} \right], \quad (38)$$

for the lower- and higher-frequency modes. Here, the subscript 0 reminds us that we have ignored $\tilde{\Omega}$. The effect of finite $\tilde{\Omega}$ can be included by perturbation theory, using Eqs. (37) and (38) as the unperturbed solutions. For the lower-frequency mode, the wave vector can be written as $(\vec{u}, \vec{v}) = (u_{\theta,0} \hat{\theta}, v_{\theta,0} \hat{\theta}) + \beta (u_{\phi,0} \hat{\phi}, v_{\phi,0} \hat{\phi})$, where β is a small coefficient. We find that β is imaginary, with

$$\text{Im}\beta = \frac{X_2}{2X} \frac{\cos \theta_q}{\sin^2 \theta_q} (1 + X)^{1/4} (1 + X \cos^2 \theta_q)^{1/4} [(1 + X \cos^2 \theta_q)^{1/2} + (1 + X \cos^2 \theta_q)^{1/2}]. \quad (39)$$

Hence, $\text{Im}\beta$ has the same sign as $\cos \theta_q$. For $q_z > 0$, the lower-frequency mode is right elliptically polarized (vice versa for $q_z < 0$). Similarly, the higher-frequency mode (the ϕ mode before perturbation) becomes left elliptically polarized, with the degree of ellipticity characterized by the same coefficient $\text{Im}\beta$.

For $\theta_q = 0$, the modes are circularly polarized, with normalized eigenvectors:

$$(u_\theta, u_\phi, v_\theta, v_\phi) = \left[\frac{(\rho_M q v_T)^{1/2} (1 + X)^{1/4}}{2}, \mp \frac{i(\rho_M q v_T)^{1/2} (1 + X)^{1/4}}{2}, \frac{i}{2(\rho_M q v_T)^{1/2} (1 + X)^{1/4}}, \frac{\pm 1}{2(\rho_M q v_T)^{1/2} (1 + X)^{1/4}} \right], \quad (40)$$

for the higher-frequency (left-circularly polarized) and lower-frequency (right-circularly polarized) modes, respectively. The opposite signs are to be taken if $\theta_q = \pi$.

Equation (39) together with Eqs. (37) and (38) allows us to obtain the Berry curvature. Here, $\vec{\Omega}_B$ has no ϕ component. For θ_q not too close to 0 or π , for the lower-frequency mode,

$$\vec{\Omega}_B \cdot \hat{\theta} = \frac{2v_T \cos^2 \theta_q}{q\omega_0 \sin^3 \theta_q}, \quad (41)$$

$$\vec{\Omega}_B \cdot \hat{q} = \frac{4v_T \cos \theta_q}{q\omega_0 \sin^4 \theta_q}. \quad (42)$$

Here, we have only kept the lowest-order finite terms and have used $\frac{1}{q^2} \frac{X_2}{X} = \frac{v_T}{2q\omega_0}$. For the higher-frequency mode, there is an extra negative sign for these formulas.

For $\theta_q = 0$, we obtain $\vec{\Omega}_B = \mp 1/q^2$ for the two modes in Eq. (40) [43].

V. DISCUSSIONS

We begin with a rough estimate for the factor Z in Eq. (21), which gives the fractional splitting in Sec. III A. Consider the case of one ion per unit cell, and let ρ_0 (dimension inverse volume) be the number of ions per unit volume, and M is the mass per unit cell. Then $Z \approx \frac{\rho_s}{\rho_0} \frac{\hbar q}{M v_T}$. (From here on, we restore the Boltzmann constant k_B and Planck constant \hbar .) Suppose that $v_T \approx 1$ km/s, $M \sim 100$ proton mass, and if the spins are polarized ($\rho_s = \rho_0$), we get $Z \sim 10^{-3}$ for a 1 meV phonon, a very large value compared with those predicted in the literature [11, 17] for other systems. For a paramagnet with

small fields, $\rho_s/\rho_0 \sim \mu_B B/k_B T$, this number will be reduced, but still not necessarily small for not-too-small fields and not-too-high temperatures.

For the parameter X in Sec. III B (note that $X \sim \frac{qv_T}{\omega_0} Z$), we obtain $X \approx 10^{-2} \frac{\rho_s}{\rho_0} \frac{(\hbar q v_T / \text{meV})^2}{(B/\text{Tesla})}$. For a 100 Tesla field and 1 meV phonon, we have a 10^{-4} splitting if we take $\rho_s = \rho_0$.

Phonons with finite Berry curvature will have an intrinsic contribution to the thermal Hall effect. Though this contribution is seemingly small and unlikely to be at least the sole mechanism for the observed thermal Hall effect for any systems, with thus extrinsic effects also called for (e.g., Refs. [41,44]), here, we provide an estimate since it is often also evaluated in the theoretical literature. Considering small external magnetic field and the simplified situation in Sec. III A, where we have two opposite circularly polarized modes, from the formulas in Refs. [13,40], we estimate [45] $\kappa_{xy}/T \sim \frac{\delta\omega}{v_T} \frac{k_B^2}{\hbar}$, where $\delta\omega$ is the typical splitting between the two oppositely polarized phonons at a given temperature, i.e., $\delta\omega \sim Z(qv_T)$, with $\hbar q v_T \sim k_B T$; thus,

$$\frac{\kappa_{xy}}{T} \sim \frac{\rho_s}{\rho_0} \frac{(k_B T)^2}{\hbar M v_T^3} \frac{k_B^2}{\hbar}.$$

We obtain that $\kappa_{xy} > 0$ (see remark below Eq. (21) and footnote [45]), independent of the sign of r . Inserting the numbers and taking again $\rho_s/\rho_0 \sim \mu_B B/k_B T$, we get

$$\kappa_{xy} \sim 10^{-8} (T/\text{K})^2 (B/\text{Tesla}) \text{W/Km}. \quad (43)$$

Here, κ_{xy} is proportional to T^2 instead of T^3 in Refs. [13,41] due to the temperature dependence of ρ_s just mentioned above. Equation (43) gives, for $B \sim 10$ Tesla and $T \sim 100$ K, $\kappa_{xy} \sim \text{mW/Km}$, a value comparable with those in, e.g., Ref. [41], and for $T \sim 30$ K, $\kappa_{xy} \sim 0.1 \text{ mW/Km}$, about an order of magnitude smaller than the peak value found experimentally for the nonmonotonic temperature-dependent κ_{xy} reported in Ref. [6]. Our number here, however, is likely to be an overestimate. The Berry curvature in our model relies on mixing between transverse modes. If we consider that rotational symmetries in crystals are discrete rather than continuous, transverse phonon modes are already split for most propagating directions. For these directions, the sound modes are only elliptically polarized rather than circularly, and the Berry curvature will be reduced. A calculation would be like what we had in Sec. IV B. Since the mixing term between the two transverse modes is $\sim Z q v_T$, if the transverse mode velocities differ by Δv_T , the curvature would be reduced by a factor $\sim Z/(\Delta v_T/v_T)$.

The mechanism discussed in this paper should be quite general, applicable to other systems so long as the pseudospin has spin and orbital degrees of freedom entangled [29] with the lowest multiplets not fully filled and not an orbital singlet, with energy well separated from the higher-energy ones, when the phonon frequencies lie within the suitable interval between these gaps. Details will differ according to the precise symmetry, and the simple vector relation Eq. (4) between the rotational matrix and the pseudospin Pauli matrices may not hold for lower symmetries. The proportionality factor r will differ from our value given, etc.; but otherwise, the induced phase factors, mixing between phonon branches, and effective Lorentz forces will remain.

Our mechanism would also be relevant for magnetically ordered systems. In this case, the coupling between the pseudospins that have been ignored so far must be considered, and our phonon-pseudospin coupling would appear as a phonon-magnon coupling. There are already quite a number of papers dealing with phonon-magnon couplings [46,47] with interesting predictions. Furthermore, mechanisms of inducing Berry curvature and chirality in the coupled phonon-magnon modes have also been proposed (e.g., Ref. [46]). However, our mechanism is of a qualitatively different nature, as it arises from the Berry phase generated from a time-dependent frame of reference of the pseudospin due to the sound mode. Instead, the mechanisms in Refs. [46,47] ultimately are both based on the modifications of the spin-spin interactions due to the phonons, with spin-orbital coupling arising from dipole-dipole interactions or magnetic anisotropy energies (see also other theoretical works [48,49] for α -RuCl₃). To what extent our present mechanism will be important for magnetically ordered systems remains to be investigated.

ACKNOWLEDGMENTS

This paper is supported by the National Science and Technology Council, Taiwan, under Grant No. MOST 110-2112-M-001-051-MY3.

APPENDIX

Here, we summarize some of the equations from Ref. [40] (hereafter MSM) and the supplemental materials of Ref. [41] (CKS-SM) that we have used in text. To simplify our notations, we shall drop labels corresponding to the components, different eigenvalues, etc.

APPENDIX A: EIGENVECTORS

After Fourier transform into wave vector \vec{q} space, $\xi_{\vec{q}}$ and $\Pi_{\vec{q}}^\dagger = \Pi_{-\vec{q}}$ satisfy the commutation relation:

$$\left[\xi_{\vec{q}}, \Pi_{\vec{q}}^\dagger \right] = i\hbar. \quad (A1)$$

Hence,

$$\begin{aligned} \beta_{\vec{q}} &= \frac{1}{\sqrt{2}} (\xi_{\vec{q}} + i\Pi_{\vec{q}}), \\ \beta_{-\vec{q}}^\dagger &= \frac{1}{\sqrt{2}} (\xi_{\vec{q}} - i\Pi_{\vec{q}}) \end{aligned} \quad (A2)$$

define a set of annihilation and creation operators. Let $\gamma_{\vec{q}}, \gamma_{-\vec{q}}^\dagger$ be instead the operators that actually diagonalize the bosonic Hamiltonian, and define the transformation matrix between $\gamma_{\vec{q}}$ and $\beta_{\vec{q}}$ as \mathcal{T}^{-1} [c.f. MSM (6)], i.e.,

$$\begin{pmatrix} \gamma_{\vec{q}} \\ \gamma_{-\vec{q}}^\dagger \end{pmatrix} = \mathcal{T}^{-1} \begin{pmatrix} \beta_{\vec{q}} \\ \beta_{-\vec{q}}^\dagger \end{pmatrix}, \quad (A3)$$

which can also be rewritten as [c.f. CKS-SM (11)]

$$\begin{pmatrix} \gamma_{\vec{q}} \\ \gamma_{-\vec{q}}^\dagger \end{pmatrix} = \mathcal{M} \begin{pmatrix} \xi_{\vec{q}} \\ \Pi_{\vec{q}} \end{pmatrix}, \quad (A4)$$

with, thus,

$$\mathcal{T}^{-1} = \frac{\mathcal{M}}{\sqrt{2}} \begin{pmatrix} 1 & 1 \\ -i & i \end{pmatrix}. \quad (\text{A5})$$

Here, \mathcal{T} satisfies [MSM (10)]:

$$\mathcal{T} \begin{pmatrix} 1 & 0 \\ 0 & -1 \end{pmatrix} \mathcal{T}^\dagger = \begin{pmatrix} 1 & 0 \\ 0 & -1 \end{pmatrix}, \quad (\text{A6})$$

and hence also the same equation with \mathcal{T} replaced by \mathcal{T}^{-1} . Equation (A5) then shows that

$$i\mathcal{M} \begin{pmatrix} 0 & 1 \\ -1 & 0 \end{pmatrix} \mathcal{M}^\dagger = \begin{pmatrix} 1 & 0 \\ 0 & -1 \end{pmatrix}, \quad (\text{A7})$$

thus equivalently CKS-SM (7).

Since we write the equation of motion for the operators $\xi_{\bar{q}}$, $\Pi_{\bar{q}}$ in the form Eq. (27) and we have defined (u, v) via Eq. (29), comparison with CKS-SM (4) and (5) shows that (u, v) are just the rows of the matrix \mathcal{M} . The normalization condition:

$$i(\bar{u} \cdot \bar{v}^* - \bar{v} \cdot \bar{u}^*) = 1, \quad (\text{A8})$$

follows from Eq. (A7).

APPENDIX B: BERRY CURVATURE

The Berry curvature for a given band n is given in MSM Eq. (34):

$$\Omega_{B,j} = i\epsilon_{jkl} \left[\begin{pmatrix} 1 & 0 \\ 0 & -1 \end{pmatrix} \frac{\partial \mathcal{T}^\dagger}{\partial q_k} \begin{pmatrix} 1 & 0 \\ 0 & -1 \end{pmatrix} \frac{\partial \mathcal{T}}{\partial q_l} \right]_{nn}. \quad (\text{B1})$$

Equation (A7) implies that

$$\begin{pmatrix} 1 & 0 \\ 0 & -1 \end{pmatrix} \mathcal{T}^\dagger \begin{pmatrix} 1 & 0 \\ 0 & -1 \end{pmatrix} = \frac{\mathcal{M}}{\sqrt{2}} \begin{pmatrix} 1 & 1 \\ -i & i \end{pmatrix}. \quad (\text{B2})$$

Substituting this into Eq. (B1), we get

$$\Omega_{B,j} = \epsilon_{jkl} \left[\frac{\partial \mathcal{M}}{\partial q_k} \begin{pmatrix} 0 & -1 \\ 1 & 0 \end{pmatrix} \frac{\partial \mathcal{M}^\dagger}{\partial q_l} \begin{pmatrix} 1 & 0 \\ 0 & -1 \end{pmatrix} \right]_{nn}. \quad (\text{B3})$$

Using that the rows of \mathcal{M} are (\bar{u}, \bar{v}) , we obtain the Berry curvature:

$$\Omega_{B,j} = -\epsilon_{jkl} \left(\frac{\partial \bar{u}}{\partial q_k} \cdot \frac{\partial \bar{v}^*}{\partial q_l} - \frac{\partial \bar{v}}{\partial q_k} \cdot \frac{\partial \bar{u}^*}{\partial q_l} \right). \quad (\text{B4})$$

Note that the right-hand side of this equation is real [50].

The Berry curvature can easily be evaluated using Eq. (B4). We display some formulas for the transverse modes, where $\bar{u} = u_\theta \hat{\theta} + u_\phi \hat{\phi}$, $\bar{v} = v_\theta \hat{\theta} + v_\phi \hat{\phi}$, with u_θ, \dots, v_ϕ depending only on q, θ but not ϕ :

$$\begin{aligned} \bar{\Omega}_B \cdot \hat{q} = & -\frac{2}{q^2} \text{Re} \left\{ \left(u_\theta v_\phi^* - u_\phi v_\theta^* \right) \right. \\ & \left. + \frac{\cos \theta}{\sin \theta} \left[-\frac{\partial}{\partial \theta} (u_\theta v_\phi^*) + \frac{\partial}{\partial \theta} (u_\phi v_\theta^*) \right] \right\}, \end{aligned} \quad (\text{B5})$$

$$\bar{\Omega}_B \cdot \hat{\theta} = -\frac{2 \cos \theta}{q \sin \theta} \text{Re} \left[\frac{\partial}{\partial q} (u_\theta v_\phi^* - u_\phi v_\theta^*) \right], \quad (\text{B6})$$

$$\begin{aligned} \bar{\Omega}_B \cdot \hat{\phi} = & -\frac{2}{q} \text{Re} \left[\frac{\partial u_\theta}{\partial q} \frac{\partial v_\theta^*}{\partial \theta} + \frac{\partial u_\phi}{\partial q} \frac{\partial v_\phi^*}{\partial \theta} \right. \\ & \left. - \frac{\partial u_\theta}{\partial \theta} \frac{\partial v_\theta^*}{\partial q} + \frac{\partial u_\phi}{\partial \theta} \frac{\partial v_\phi^*}{\partial q} \right]. \end{aligned} \quad (\text{B7})$$

In Eqs. (B5)–(B7), we have dropped the subscripts q of θ_q to simplify the notation.

-
- [1] C. Strohm, G. L. J. A. Rikken, and P. Wyder, *Phys. Rev. Lett.* **95**, 155901 (2005).
- [2] T. Ideue, T. Kurumaji, S. Ishiwata, and Y. Tokura, *Nat. Mater.* **16**, 797 (2017).
- [3] Y. Kasahara, K. Sugii, T. Ohnishi, M. Shimozawa, M. Yamashita, N. Kurita, H. Tanaka, J. Nasu, Y. Motome, T. Shibauchi *et al.*, *Phys. Rev. Lett.* **120**, 217205 (2018).
- [4] Y. Kasahara, T. Ohnishi, Y. Mizukami, O. Tanaka, S. Ma, K. Sugii, N. Kurita, H. Tanaka, J. Nasu, Y. Motome *et al.*, *Nature (London)* **559**, 227 (2018).
- [5] G. Grissonnanche, A. Legros, S. Badoux, E. Lefrançois, V. Zatzko, M. Lizaïre, F. Laliberté, A. Gourgout, J.-S. Zhou, S. Pyon *et al.*, *Nature (London)* **571**, 376 (2019).
- [6] R. Henrich, M. Roslaov, A. Isaeva, T. Doert, W. Brenig, B. Büchner, and C. Hess, *Phys. Rev. B* **99**, 085136 (2019).
- [7] X. Li, B. Fauqué, Z. Zhu, and K. Behnia, *Phys. Rev. Lett.* **124**, 105901 (2020).
- [8] M.-E. Boulanger, G. Grissonnanche, S. Badoux, A. Allaire, E. Lefrançois, A. Legros, A. Gourgout, M. Dion, C. H. Wang, X. H. Chen *et al.*, *Nat. Commun.* **11**, 5325 (2020).
- [9] S. Sim, H. Yang, H.-L. Kim, M. J. Coak, M. Itoh, Y. Noda, and J.-G. Park, *Phys. Rev. Lett.* **126**, 015901 (2021).
- [10] É. Lefrançois, G. Grissonnanche, J. Baglo, P. Lampen-Kelley, J.-Q. Yan, C. Balz, D. Mandrus, S. E. Nagler, K. Kim, Y.-J. Kim *et al.*, *Phys. Rev. X* **12**, 021025 (2022).
- [11] D. M. Juraschek and N. A. Spaldin, *Phys. Rev. Mater.* **3**, 064405 (2019).
- [12] C. A. Mead and D. G. Truhlar, *J. Chem. Phys.* **70**, 2284 (1979).
- [13] T. Qin, J. Zhou, and J. Shi, *Phys. Rev. B* **86**, 104305 (2012).
- [14] T. Saito, K. Misaki, H. Ishizuka, and N. Nagaosa, *Phys. Rev. Lett.* **123**, 255901 (2019).
- [15] O. Bistoni, F. Mauri, and M. Calandra, *Phys. Rev. Lett.* **126**, 225703 (2021).
- [16] D. Saporov, B. Xiong, Y. Ren, and Q. Niu, *Phys. Rev. B* **105**, 064303 (2022).
- [17] J. Bonini, S. Ren, D. Vanderbilt, M. Stengel, C. E. Dreyer, and S. Coh, *Phys. Rev. Lett.* **130**, 086701 (2023).
- [18] C. A. Mead, *Rev. Mod. Phys.* **64**, 51 (1992).
- [19] S. Baroni, S. de Gironcoli, A. Dal Corso, and P. Giannozzi, *Rev. Mod. Phys.* **73**, 515 (2001); F. Giustino, *ibid.* **89**, 015003 (2017).
- [20] F. Wilczek and A. Zee, *Phys. Rev. Lett.* **52**, 2111 (1984).
- [21] M. Stone, *Phys. Rev. D* **33**, 1191 (1986).

- [22] N. Goldman, G. Juzeliūnas, P. Öhberg, and I. B. Spielman, *Rep. Prog. Phys.* **77**, 126401 (2014).
- [23] C. Kittel, *Phys. Rev.* **110**, 836 (1958).
- [24] B. J. Kim, H. Jin, S. J. Moon, J.-Y. Kim, B.-G. Park, C. S. Leem, J. Yu, T. W. Noh, C. Kim, S.-J. Oh *et al.*, *Phys. Rev. Lett.* **101**, 076402 (2008).
- [25] B. J. Kim, H. Ohsumi, T. Komesu, S. Sakai, T. Morita, H. Takagi, and T. Arima, *Science* **323**, 1329 (2009).
- [26] A. Shitade, H. Katsura, J. Kuneš, X.-L. Qi, S.-C. Zhang, and N. Nagaosa, *Phys. Rev. Lett.* **102**, 256403 (2009).
- [27] G. Jackeli and G. Khaliullin, *Phys. Rev. Lett.* **102**, 017205 (2009).
- [28] For Sr_2IrO_4 , the separation between the $j_{\text{eff}} = \frac{1}{2}$ and $\frac{3}{2}$ manifold is several hundred meV according to Ref. [24].
- [29] T. Takayama, J. Chaloupka, A. Smerald, G. Khaliullin, and H. Takagi, *J. Phys. Soc. Jpn.* **90**, 062001 (2021).
- [30] P. Thalmeier and P. Fulde, *Z. Phys. B* **26**, 323 (1977).
- [31] G. Schaack, *Z. Phys. B* **26**, 49 (1977).
- [32] H. Capellmann, S. Lipinski, and K. U. Neumann, *Z. Phys. B* **75**, 323 (1989).
- [33] H. Capellmann and S. Lipinski, *Z. Phys. B* **83**, 199 (1991).
- [34] E. Du Trémolet de Lacheisserie, *Magnetostriction: Theory and Applications of Magnetoelasticity* (CRC Press, Boca Raton, 1993).
- [35] Our choice of phase factors in Eq. (1) contains an overall extra factor $-i$ compared with Ref. [26]. This is to guarantee the time-reversal symmetry mentioned. See also the remark [36] below.
- [36] The choice in Ref. [27] would correspond to removing the factors $\mp i$ in Eq. (1). We would have instead $L_z = -\frac{2}{3}\tau_z$, but $L_{x,y} = +\frac{2}{3}\tau_{x,y}$ and similarly for the spin. Similarly, the choice in Ref. [25] would not yield a simple vector relation as in Eq. (2).
- [37] L. D. Landau and E. M. Lifshitz, *Theory of Elasticity*, Course of Theoretical Physics, Vol. 7 (Pergamon Press, Oxford, 1970).
- [38] The isotropic compression can cause an overall shift in energy, but that would be common to both energy levels in Eq. (5), while the anisotropy can cause virtual transition to higher energy levels. In neither case can these generate a linear coupling to $\vec{\tau}$ or \vec{B} , which are vectors. We shall be confining ourselves to effects that are first order in \vec{B} .
- [39] A. Altland and B. Simons, *Condensed Matter Field Theory* (Cambridge University Press, Cambridge, 2006).
- [40] R. Matsumoto, R. Shindou, and S. Murakami, *Phys. Rev. B* **89**, 054420 (2014).
- [41] J.-Y. Chen, S. A. Kivelson, and X.-Q. Sun, *Phys. Rev. Lett.* **124**, 167601 (2020).
- [42] D. M. Juraschek, T. Neuman, and P. Narang, *Phys. Rev. Res.* **4**, 013129 (2022).
- [43] $\vec{\Omega}_B \cdot \hat{\phi}$ vanishes by symmetry, but Eq. (40) itself is not sufficient to evaluate the other two components since information near small and finite θ 's are needed. At small θ , writing the correction factors as $(1 + c_1\theta^2)$ with $c_{1,2,3,4}$, etc., for the four components in Eq. (40), $c_1 + c_2 + c_3 + c_4 = 0$ due to normalization. This implies the results given in text.
- [44] M. Mori, A. Spencer-Smith, O. P. Sushkov, and S. Maekawa, *Phys. Rev. Lett.* **113**, 265901 (2014).
- [45] This intrinsic contribution is a sum over phonon modes weighted by thermal factors for two circularly polarized modes with opposite Berry curvatures, hence opposite contributions to κ_{xy} . Note that, due to the remark after Eq. (21), the lower frequency modes for both $q_z \geq 0$ have $\vec{\Omega}_B \cdot \hat{z} < 0$ and so adds. Hence, $\kappa_{xy}/T \sim q^3 \times (1/q^2) \times (\hbar\delta\omega/k_B T)(k_B^2/\hbar)$, where the first factor is from the q integral, the second from the Berry curvature, and the third from the difference in occupation numbers of the two modes, and each of these factors can be replaced by the typical value at a given temperature T . This estimate also follows from dimensional analysis (κ_{xy}/T has the dimension of inverse length apart from the factor k_B^2/\hbar). A more detailed calculation using the formulas in Refs. [13,40] yields the same result except a numerical factor of order 1.
- [46] R. Takahashi and N. Nagaosa, *Phys. Rev. Lett.* **117**, 217205 (2016).
- [47] P. Delugas, O. Baseggio, I. Timrov, S. Baroni, and T. Gorni, *Phys. Rev. B* **107**, 214452 (2023).
- [48] M. Ye, R. M. Fernandes, and N. B. Perkins, *Phys. Rev. Res.* **2**, 033180 (2020).
- [49] S. Li, H. Yan, and A. H. Nevidomskyy, [arXiv:2301.07401](https://arxiv.org/abs/2301.07401).
- [50] CKS-SM (13) seems to contain some typos. Their expression is imaginary.